

## Trastuzumab Has Preferential Activity against Breast Cancers Driven by HER2 Homodimers

Ritwik Ghosh<sup>1</sup>, Archana Narasanna<sup>1</sup>, Shizhen Emily Wang<sup>2</sup>, Shuying Liu<sup>4,5</sup>, Anindita Chakrabarty<sup>1</sup>, Justin M. Balko<sup>1</sup>, Ana María González-Angulo<sup>4,5</sup>, Gordon B. Mills<sup>4,6</sup>, Elicia Penuel<sup>7</sup>, John Winslow<sup>7</sup>, Jeff Sperinde<sup>7</sup>, Rajiv Dua<sup>7</sup>, Sailaja Pidaparthy<sup>7</sup>, Ali Mukherjee<sup>7</sup>, Kim Leitzel<sup>8</sup>, Wolfgang J. Kostler<sup>9</sup>, Allan Lipton<sup>8</sup>, Michael Bates<sup>7</sup>, and Carlos L. Arteaga<sup>1,2,3</sup>

### Abstract

In breast cancer cells with *HER2* gene amplification, HER2 receptors exist on the cell surface as monomers, homodimers, and heterodimers with EGFR/HER3. The therapeutic antibody trastuzumab, an approved therapy for HER2<sup>+</sup> breast cancer, cannot block ligand-induced HER2 heterodimers, suggesting it cannot effectively inhibit HER2 signaling. Hence, HER2 oligomeric states may predict the odds of a clinical response to trastuzumab in HER2-driven tumors. To test this hypothesis, we generated nontransformed human MCF10A mammary epithelial cells stably expressing a chimeric HER2–FKBP molecule that could be conditionally induced to homodimerize by adding the FKBP ligand AP1510, or instead induced to heterodimerize with EGFR or HER3 by adding the heterodimer ligands EGF/TGF $\alpha$  or heregulin. AP1510, EGF, and heregulin each induced growth of MCF10A cells expressing HER2–FKBP. Trastuzumab inhibited homodimer-mediated but not heterodimer-mediated cell growth. In contrast, the HER2 antibody pertuzumab, which blocks HER2 heterodimerization, inhibited growth induced by heregulin but not AP1510. Lastly, the HER2/EGFR tyrosine kinase inhibitor lapatinib blocked both homodimer- and heterodimer-induced growth. AP1510 triggered phosphorylation of Erk1/2 but not AKT, whereas trastuzumab inhibited AP1510-induced Erk1/2 phosphorylation and Shc-HER2 homodimer binding, but not TGF $\alpha$ -induced AKT phosphorylation. Consistent with these observations, high levels of HER2 homodimers correlated with longer time to progression following trastuzumab therapy in a cohort of patients with HER2-overexpressing breast cancer. Together, our findings confirm the notion that HER2 oligomeric states regulate HER2 signaling, also arguing that trastuzumab sensitivity of homodimers may reflect their inability to activate the PI3K (phosphoinositide 3-kinase)/AKT pathway. A clinical implication of our results is that high levels of HER2 homodimers may predict a positive response to trastuzumab. *Cancer Res*; 71(5): 1871–82. ©2011 AACR.

### Introduction

ErbB receptors are transmembrane tyrosine kinases comprising four members: ErbB1/EGFR, ErbB2/HER2, ErbB3/HER3, and ErbB4/HER4 (1). Dysregulation of ErbB expression has been associated with cancers of the lung, breast, head and

neck, gastrointestinal tract, ovary, brain, and prostate (2–4). *HER2* gene amplification and protein overexpression, present in about 25% of invasive breast cancers (5), are associated with poor patient prognosis. In HER2-overexpressing breast cancer cells, HER2 is present in a complex equilibrium of preassociated active and inactive homodimers, heterodimers, and monomers on the cell surface (6). Recruitment of HER2 to its coreceptors potentiates signaling by HER2-containing heterodimers (7, 8). In HER2-overexpressing cells, the kinase-impaired HER3 coreceptor is the main adaptor that directly couples to the phosphatidylinositol-3 kinase PI3K (phosphoinositide 3-kinase)/AKT pathway (9). HER2 overexpression also activates the Ras/Raf/MEK (MAP/ERK kinase)/MAPK (mitogen activated protein kinase) pathway via the recruitment of the adaptor proteins Grb2 and Shc (10).

Trastuzumab, an antibody against the ectodomain of HER2, is approved for the treatment of HER2-overexpressing breast cancer (11, 12). Overall, trastuzumab is clinically effective but a significant proportion of HER2-overexpressing breast cancer patients either do not respond or eventually become resistant to trastuzumab (13–15). Predictive assays to reliably identify

**Authors' Affiliations:** Departments of <sup>1</sup>Medicine and <sup>2</sup>Cancer Biology, and <sup>3</sup>Breast Cancer Research Program, Vanderbilt-Ingram Cancer Center; Vanderbilt University, Nashville, Tennessee; Departments of <sup>4</sup>Systems Biology, <sup>5</sup>Breast Medical Oncology, and <sup>6</sup>Gynecological Medical Oncology, University of Texas MD Anderson Cancer Center, Houston, Texas; <sup>7</sup>Monogram Biosciences Inc., South San Francisco, California; <sup>8</sup>Division of Hematology–Oncology, Penn State/Hershey Medical Center, Hershey, Pennsylvania; and <sup>9</sup>Department of Medicine, Medical University of Vienna, Vienna, Austria

**Note:** Supplementary data for this article are available at Cancer Research Online (<http://cancerres.aacrjournals.org/>).

**Corresponding Author:** Carlos L. Arteaga, Division of Oncology, VUMC 2220 Pierce Avenue, 777 PRB Nashville, TN 37232-6307. Phone: 615-936-3524; Fax: 615-936-1790; E-mail: carlos.l.arteaga@vanderbilt.edu

doi: 10.1158/0008-5472.CAN-10-1872

©2011 American Association for Cancer Research.

HER2-overexpressing cancers that will respond or not to existing anti-HER2 therapy are not yet available.

Several studies have reported on possible mechanisms of resistance to trastuzumab. For example, amplification of PI3K signaling due to loss of lipid phosphatase PTEN or expression of *PIK3CA*-activating mutations is associated with lower response to trastuzumab (16, 17). Another pathway to resistance is overexpression of ligands of EGFR and HER3/4 (18). This is consistent with structural and cellular data using ErbB receptor ectodomains, which show that trastuzumab is unable to block ligand-induced EGFR/HER2 and HER2/HER3 heterodimers (19, 20). Thus, we hypothesized that HER2-overexpressing breast cancers containing high levels of EGFR/HER2 and HER2/HER3 heterodimers, surrogate markers of ErbB ligand-induced transactivation of HER2, will exhibit a lower response to trastuzumab compared with HER2<sup>+</sup> tumors with undetectable or low levels of these heterodimers. In order to identify differential signaling induced by HER2-containing homo- and heterodimers and to develop potential biomarkers of response to trastuzumab, we have developed a cell system in which HER2 dimerization can be conditionally regulated.

## Materials and Methods

### Generation of MCF10A cells expressing HER2–FKBP–HA chimeric receptors

Vector-expressing HER2–FKBP–HA chimera was generated as described in Supplementary Methods (21). Retroviruses expressing HER2 chimeras were produced by transfecting Phoenix-Ampho cells, using published methods (22), and then utilized to transduce MCF10A human mammary epithelial cells. Stably transfected cells were selected in 1 mg/mL G418 (22).

### Cell culture, receptor ligands, and inhibitors

MCF10A–HER2–FKBP–HA cells were maintained in DMEM/F-12 medium supplemented with epidermal growth factor (EGF; 20 ng/mL; Invitrogen/Gibco), cholera toxin (100 ng/mL; Sigma), hydrocortisone (500 ng/mL; Sigma), insulin (10 µg/mL; Invitrogen/Gibco), and 5% horse serum (HS; Hyclone). For experiments examining receptor dimerization and signaling, cells were treated with ligands ± inhibitors, as described in Supplementary Methods.

### Three-dimensional Matrigel growth assay

About  $5 \times 10^3$  cells/well were seeded in 8-well chamber slides in DMEM/F-12 medium supplemented with cholera toxin, hydrocortisone, insulin and 2% HS on growth factor-reduced Matrigel (BD Biosciences), as described (23). Ligands ± inhibitors were added at the time of seeding cells and replenished along with fresh media every 3 days. Acinar growth was quantified as described in Supplementary Methods.

### Cross-linking, immunoprecipitation, and immunoblotting

Cells were cross-linked with bis(sulfosuccinimidyl)suberate (BS<sup>3</sup>), as described (24). After cross-linking, cells were lysed in

Triton lysis buffer, followed by immunoprecipitation with an HER2 antibody Ab8 (Neomarkers), as described (24, 25). For immunoblot analysis, cells were lysed in 1% NP-40 buffer containing protease and phosphatase inhibitors. Samples were sonicated for 10 seconds and centrifuged at 14,000 rpm for 5 minutes at 4°C; protein concentrations were quantitated using the BCA assay (Pierce). Immunoprecipitations were done with HER3 or HA antibodies, followed by protein G (for HA) or protein A (for HER3) beads (Sigma), as described (26). Immune complexes and whole cell lysates were subjected to SDS-PAGE and transferred onto nitrocellulose membrane. Primary antibodies for immunoblotting included total AKT, S473-pAKT, T308-pAKT, HA, pErk1/2, Erk1/2 (Cell Signaling), HER3, EGFR (Santa Cruz Biotechnology), HER2 (Neomarkers), actin (Sigma), and the 4G10 phosphotyrosine antibody (Millipore).

### Cell-surface biotinylation

The Cell Surface Protein Isolation kit (Pierce) was used for biotinylation studies according to the manufacturer's protocol and as described in Supplementary Methods.

### Gene expression profiling

RNA was isolated from cells grown on 100-mm dishes, using the ToTALLY RNA kit from Ambion following the manufacturer's protocol. Synthesis of cRNA target, its hybridization to Human Gene 1.0 ST microarrays, and scanning of those arrays was done using Affymetrix GeneChip products and reagents at the Vanderbilt Microarray Shared Resource. Data were analyzed as described in Supplementary Methods (27). Raw data are available in GEO (accession # GSE22288).

### Reverse-phase protein array

Cell lysates were prepared for reverse-phase protein array (RPPA), as described previously (28–30). RPPA was done, and data were analyzed as described in Supplementary Methods.

### Fluorescent proximity-based antibody-dependent dimer detection (VeraTag) assay

VeraTag assays with tumor sections and cells treated with receptor ligands were carried out as described previously (25) and in Supplementary Methods.

### Study patient population

A description of clinical characteristics of the study population is provided in Table 1. Response to treatment was documented by review of all imaging studies according to Southwest Oncology Group (SWOG) criteria, as previously described (31). Further details are provided in Supplementary Methods.

### Statistical analysis

Clinical cutoffs for HER2 homodimer levels (HER22) were determined by positional scanning analysis and selection of the cutoff associated with the lowest *P* value for time to progression (TTP). Correlation of HER22 levels with clinical outcome was determined as described in Supplementary Methods.

**Table 1.** Patient/cohort characteristics

Characteristic	Number (range, %)
Total patients	101
Mean follow-up, mo	34 (11.8–77.9)
Mean age	55.4 (27.6–85.4)
H2T (> cutoff)	69 (68)
Number of metastatic sites	
<3	59 (59)
≥3	42 (41)
Hormonal status	
ER <sup>+</sup> PR <sup>+</sup>	17 (17)
ER <sup>+</sup> PR <sup>-</sup>	18 (18)
ER <sup>-</sup> PR <sup>+</sup>	3 (3)
ER <sup>-</sup> PR <sup>-</sup>	61 (60)
Unknown	2 (2)
HER2 status	
2+	5
FISH <sup>+</sup>	5
3+	94
FISH <sup>+</sup>	71
FISH <sup>-</sup>	21
FISH unknown	2
Unknown	2
FISH <sup>+</sup>	2
Treatment	
Trastuzumab + chemotherapy	89 (88)
Trastuzumab only	12 (12)
Line of chemotherapy	
First	74 (74)
Second	17 (17)
Third	8 (8)
Unknown	2 (2)

Abbreviations: ER, estrogen receptor; PR, progesterone receptor.

## Results

### Cell system with controlled ErbB receptor dimerization

We generated HER2 chimeras containing the full-length human HER2 sequence fused to HA-tagged ligand-binding domain of FK506-binding protein (FKBP; Fig. 1A). A retroviral vector encoding for this chimera was stably transduced into MCF10A human mammary epithelial cells to produce MCF10A/HER2/FKBP/HA cells (henceforth FKBP–HA cells). Immunoprecipitation of cross-linked HER2 confirmed induction of HER2 homodimer formation following addition of synthetic FKBP ligand AP1510 (Fig. 1B, left). Sustained AP1510-induced tyrosine phosphorylation of HER2 (24 hours) was confirmed by precipitation with an HA antibody followed by p-Tyr immunoblot (Fig. 1B, right). Western blot analyses revealed activation of pErk1/2 but not T308- or S473-pAKT following AP1510 treatment (Fig. 1C, left). To confirm that AP1510-induced pErk1/2 does not involve EGFR activation, FKBP–HA cells were treated with receptor ligands ± the

EGFR inhibitor erlotinib. Erlotinib blocked TGF $\alpha$  (EGFR ligand)-induced but not AP1510- or heregulin (HER3 ligand)-induced pErk1/2 (Fig. 1C, right). These results suggest that HER2 homodimers and HER2-containing heterodimers preferentially engage different downstream signaling effectors with HER2 homodimers activating the Erk1/2 but not the AKT pathway.

Since we used full-length human HER2 to produce the HER2–FKBP–HA chimera, we reasoned the transfected HER2 receptor should retain its ability to dimerize with ligand-stimulated EGFR and HER3. To test this, FKBP–HA cells were treated with AP1510, heregulin, and TGF $\alpha$ . Immunoprecipitation with HER3 antibody followed by HA immunoblot indicated heregulin-enhanced HER2/HER3 heterodimer formation compared with AP1510-treated cells (Fig. 1D, right). Similarly, precipitation with HA antibody followed by EGFR immunoblot analyses showed that TGF $\alpha$  but not AP1510 stimulated the formation of HER2/EGFR heterodimers (Fig. 1D, left).

### Cell growth following HER2 homodimerization is inhibited by trastuzumab

We next examined growth of FKBP–HA cells in response to different ligands. Wild-type MCF10A cells form polarized, single-cell, quiescent acini in 3-dimensional (3D) basement membrane. However, in MCF10A cells transfected with an HER2 chimera, activation of HER2 results in enhanced proliferation, reduction in apoptosis of centrally located cells, disruption of tight junctions and polarity, and induction of acinar expansion without invasion into surrounding matrix (23, 32). Like in these previous reports, all three ligands, AP1510, EGF, and heregulin, induced formation of invasive FKBP–HA cell acini in growth factor-reduced 3D Matrigel while cells in which HER2 had not been activated did not grow (Fig. 2A). Trastuzumab completely inhibited AP1510-stimulated but not EGF- or heregulin-stimulated growth. Pertuzumab, an antibody that binds to the heterodimerization domain of HER2 (33), inhibited acinar growth induced by heregulin but not by AP1510 or EGF. Lapatinib, a dual inhibitor of the HER2 and EGFR tyrosine kinases, blocked EGF-, heregulin-, and AP1510-induced growth (Fig. 2). These results confirm that growth of FKBP–HA cells as a result of ligand-induced HER2 heterodimerization is insensitive to trastuzumab.

### Differential signaling by HER2-containing homo- and heterodimers

HER2 homodimers activated Erk1/2 but not PI3K/AKT (Fig. 1C). On the other hand, TGF $\alpha$ -induced HER2/EGFR heterodimers and activated both AKT and Erk1/2 (Supplementary Fig. 1A). Heregulin induced HER2/HER3 complex formation but the effect on AKT and Erk1/2 was not pronounced, presumably due to low levels of HER3 present in FKBP–HA cells (Supplementary Fig. 1A). To further characterize dimer-induced signaling, we carried out RPPA assays on cells treated with receptor ligands over a time course. We used 96 antibodies against total and phosphorylated proteins, using methods analogous to high-throughput dot blotting (29, 30).

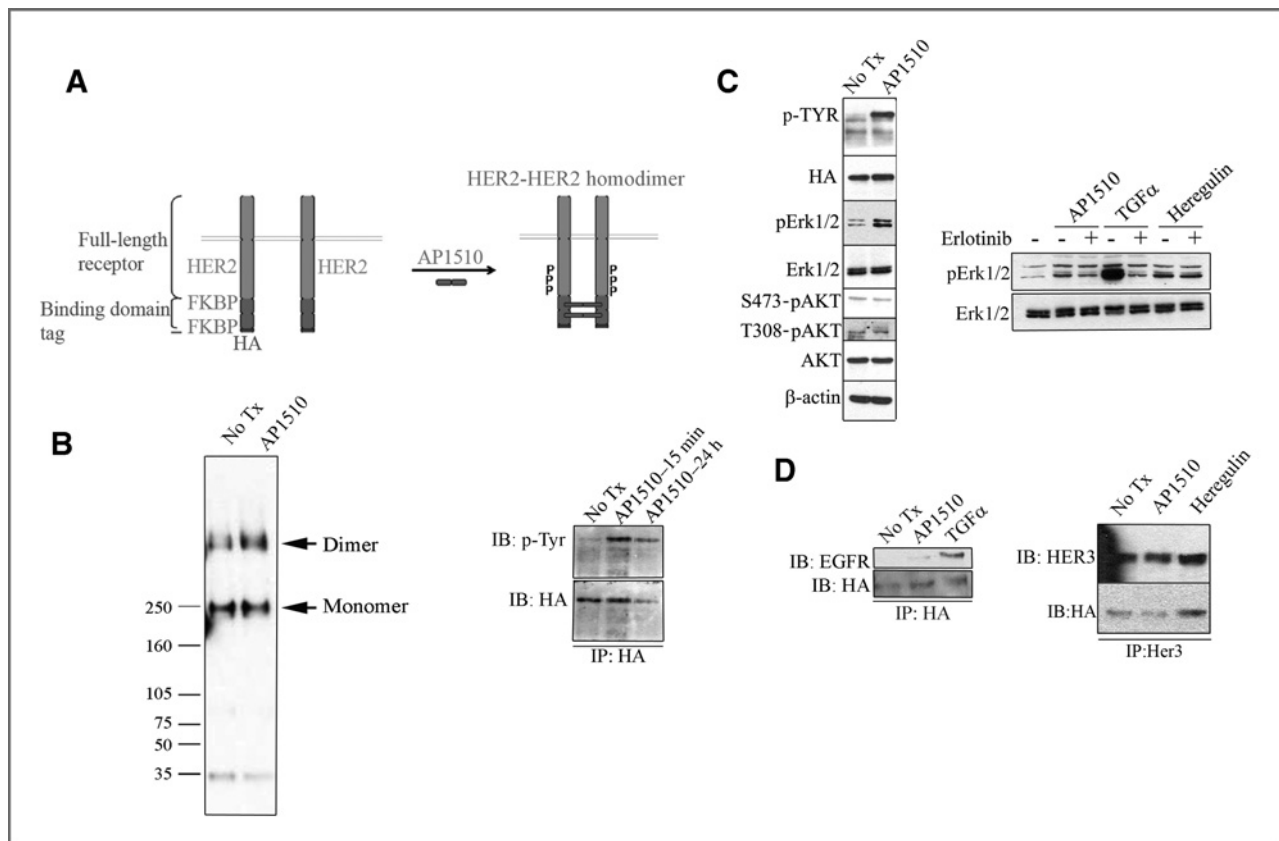


**Figure 1.** Cell system with controlled ErbB receptor dimerization. **A**, cartoon showing cell system for controlled ErbB2 dimerization. **B**, left, cross-linking assay to confirm AP1510-induced HER2 homodimerization. Cross-linking was done following 15 minutes of AP1510 stimulation. HER2 was immunoprecipitated; immune complexes were subjected to SDS-PAGE and immunoblotted with an HER2 antibody. Molecular weights in kilodalton are indicated to the left. Right, FKBP-HA cells were treated with AP1510 for 15 minutes or 24 hours. HA-tagged HER2 was immunoprecipitated and pull-downs were subjected to SDS-PAGE and immunoblotted with a p-Tyr antibody. **C**, FKBP-HA cells were treated with AP1510 alone (left) or AP1510, TGF $\alpha$ , or heregulin  $\pm$  erlotinib (1  $\mu$ mol/L) for 1 hour (right). Protein extracts were prepared as indicated in Materials and Methods and subjected to SDS-PAGE and immunoblotted with the antibodies indicated to the left of each panel. **D**, binding of chimeric HER2 to ligand-stimulated EGFR and HER3. FKBP-HA cells were stimulated with AP1510 or TGF $\alpha$  (left) or with AP1510 or heregulin (right), each for 15 minutes. Cell lysates were precipitated with HA (left) or HER3 (right) antibodies, and immune complexes were separated by SDS-PAGE followed by immunoblot analysis with HA, EGFR, or HER3 antibodies as indicated.

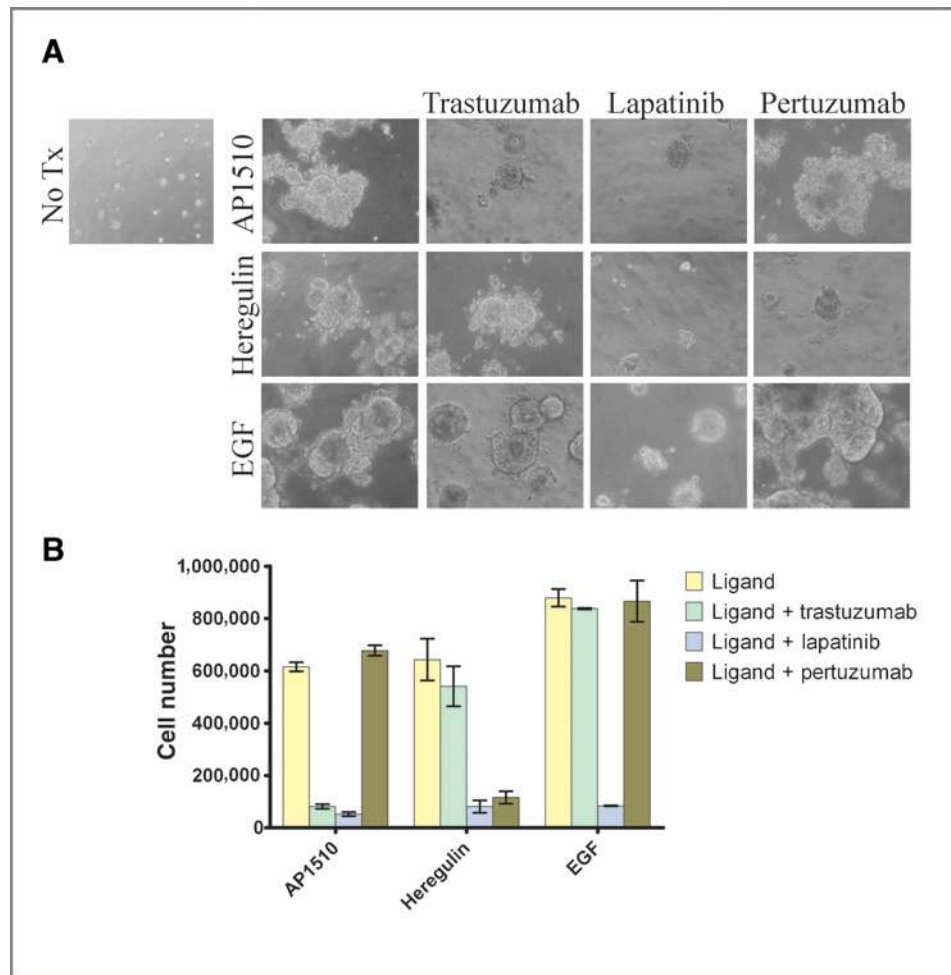
We undertook step-down quadratic regression analysis for pattern recognition in time course studies (ref. 34; Supplementary Fig. 1B) and significance analysis using the Significance Analysis of Microarray (SAM) algorithm [false discovery rate (FDR) = 0%; Fig. 3A] on RPPA from ligand-stimulated cells. We also studied activation of signaling downstream of the PI3K/AKT (as phosphorylation of AKT, GSK3, mTOR, p70S6, 4EBP, and S6) and MAPK (as phosphorylation of MAPK, MEK, Ser<sup>118</sup> ER $\alpha$ , and JNK) pathways (35). RPPA assays confirmed that TGF $\alpha$  induced both PI3K and MAPK pathways, whereas AP1510 stimulated only the MAPK pathway as measured by activation of signaling downstream of these two pathways (Supplementary Fig. 2). RPPA analysis also confirmed previously reported association between HER2/HER3 heterocomplex formation and activation of Src measured as phosphorylation at Y416 (Fig. 3A, iii and iv; refs. 36, 37). This is consistent with a previous report in which heregulin induced recruitment of HER3 to an HER2-Src (36). Furthermore, 2 studies have reported on heregulin-induced activation of HER3/HER2 dimers resulting in Src kinase activation (37,

38). In contrast to HER3/HER2 heterodimers, RPPA analysis showed that HER2 homodimers and HER2/EGFR heterodimers did not induce Src.Y416 phosphorylation.

We next generated microarrays on RNA isolated from cells treated with receptor ligands. Analysis of transcriptional events induced by activation of ErbB dimers indicated that unique genes were regulated by HER2/HER2, HER2/EGFR, and HER2/HER3 dimers (Fig. 3B). SAM identified 323 genes (FDR = 0%) that are significantly different among the 4 treatment groups (Supplementary Fig. 3). Furthermore, gene expression data from triplicate RNA samples from different treatments cluster into distinct groups, indicating that HER2-containing dimers activate unique transcriptional profiles (Fig. 3C). A comparative analysis (Ingenuity Pathway Software) of the effect of activated ErbB receptors on canonical pathways involved in human malignancies revealed that HER2/HER2 and HER2/EGFR, but not HER2/HER3, can modulate the "cell cycle: G<sub>2</sub>/M DNA damage checkpoint regulation" pathway (Fig. 3D). Cyclin B1 (CCNB1), a known regulator of G<sub>2</sub>/M transition (39), is associated with aggressive pheno-



**Figure 2.** Cell growth following HER2 homodimerization is inhibited by trastuzumab. A, cells ( $5 \times 10^3$ /well) were seeded in DMEM/F-12 media with cholera toxin, hydrocortisone, insulin, and 2% HS. Cells were treated with receptor ligands AP1510 (1  $\mu$ mol/L), EGF (5 ng/mL), heregulin (10 ng/mL)  $\pm$  trastuzumab (20  $\mu$ g/mL), and lapatinib (1  $\mu$ mol)  $\pm$  pertuzumab (20  $\mu$ g/mL) for 12 days. Media, ligands, and inhibitors were replenished every 3 days. B, Matrigel was dissolved (see Methods) and cells were counted to quantify 3D cell growth. Each bar graph represents the mean  $\pm$  SD of duplicate wells.



type in breast cancer (40). Interestingly, our RPPA data show that HER2 homodimers and HER2/EGFR heterodimers, but not HER2/HER3 heterodimers, enhance CCNB1 expression (Fig. 3A, i, ii, and vi), thus concurring with the Ingenuity Pathway analysis.

In a recent study, hierarchical clustering of gene expression data from 58 HER2-overexpressing patients identified a 158-gene signature that can distinguish between patients with poor and good prognoses (27). To examine if this HER2-derived prognostic predictor (HDPP) gene signature correlated with the ligand-induced RNA expression signatures, we merged our microarray data with the "good prognosis" and "poor prognosis" centroids (27). Complete hierarchical clustering was done using 139 of 158 centroid genes (due to platform representation). Consistent with broader induction of signaling, the TGF $\alpha$ -induced signature clustered with the poor prognostic signature whereas AP1510-induced signature clustered with the good prognostic signature (Supplementary Fig. 4). Although heregulin-treated cells showed a trend toward increased similarity with the poor prognostic signature, they clustered with the good prognostic signature (Supplementary Fig. 4). This analysis further supports differential molecular outputs of different HER2-containing dimers and is

compatible with EGFR/HER2 heterodimers being the key complex associated with a worse prognosis.

#### Trastuzumab blocks HER2 homodimer- but not heterodimer-induced Erk1/2 activity

We next sought to determine if trastuzumab selectively blocks signaling downstream of the ErbB receptor network. Immunoblot analysis of lysates from ligand-stimulated FKBP-HA cells showed that trastuzumab blocked AP1510-induced but not TGF $\alpha$ - or heregulin-induced pErk1/2. Consistent with the cell growth data, trastuzumab did not inhibit TGF $\alpha$ - or heregulin-induced pAKT (Fig. 4A). Cell-surface biotinylation studies indicated that trastuzumab can induce similar HER2 internalization in AP1510-, TGF $\alpha$ -, and heregulin-treated cells (Fig. 4B), suggesting that the selective inhibitory effect of trastuzumab on Erk1/2 was not due to a differential effect on receptor binding and subsequent receptor downregulation from the cell surface.

The adaptor protein Shc is recruited by HER2 to induce MAPK signaling (10); thus, we examined whether trastuzumab impaired the engagement of Shc by activated HER2. Chimeric HER2 was precipitated using an HA antibody from cells treated with different ligands  $\pm$  trastuzumab followed by

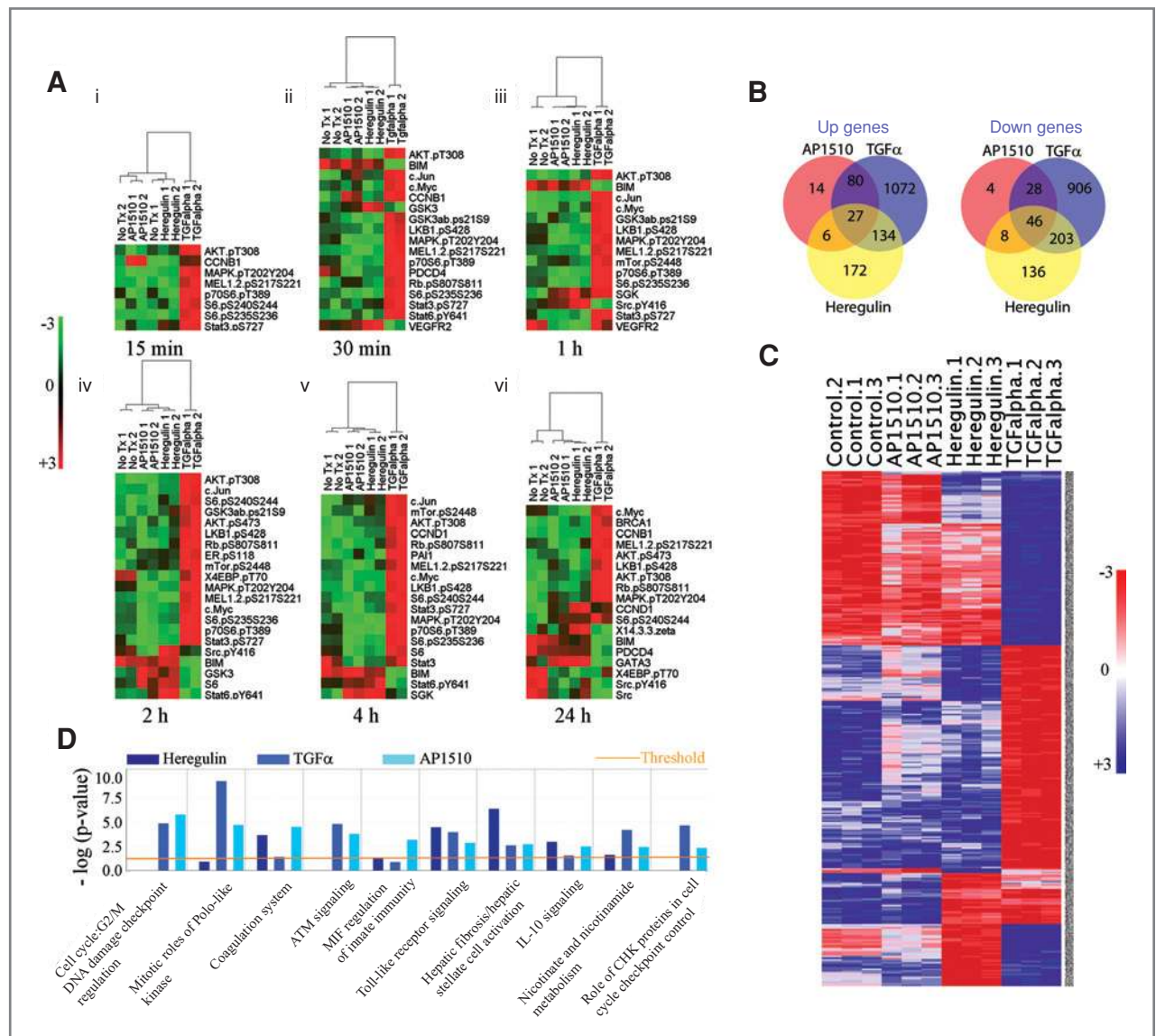


**Figure 3.** RPPA and RNA microarrays. Differential signaling induced by ErbB2-containing dimers. A, protein lysates were prepared from cells treated with AP1510, TGF $\alpha$ , or heregulin for 0, 0.25, 0.50, 1, 2, 4, and 8 hours, as indicated in Materials and Methods. Hierarchical clustering was done with proteins that underwent statistically significant change (identified using the SAM algorithm with an FDR of 0%) compared with control for each time point. Specific proteins are indicated to the right of each panel. B–D, RNA was isolated from control, AP1510-, TGF $\alpha$ -, or heregulin-treated cells (48 hours) and subjected to microarray analysis as indicated in Materials and Methods. B, Venn diagram was drawn with up- or downregulated genes with each treatment. Only genes that underwent at least a 1.5-fold change ( $P < 0.05$ ) were included. C, hierarchical clustering was done with a gene list generated by the SAM algorithm (FDR 0%) to identify differential gene sets induced by HER2 homo- and heterodimers. D, Ingenuity Pathway analysis to identify distinct physiologic pathways modulated by HER2 homo- and heterodimers. The Y-axis represents Fisher's exact test  $P$  value. A Y-axis value of greater than 1.3 (yellow, line threshold) is equivalent to a value of  $P < 0.05$ .

Shc immunoblot analysis. AP1510, TGF $\alpha$ , and heregulin enhanced the association of HER2–FKBP–HA with the 66-, 52-, and 46-kDa forms of Shc. Treatment with trastuzumab dissociated Shc only from AP1510- but not from TGF $\alpha$ - or heregulin-stimulated cells (Fig. 4A, bottom two panels). This result suggests that trastuzumab selectively blocks HER2 homodimer-induced Erk1/2 by causing a dissociation of Shc from HER2 homodimers. We next postulated that inhibition of MAPK should phenocopy the effect of trastuzumab on AP1510-

stimulated FKBP–HA cells and that EGFR/HER2 heterodimer-induced cell growth should be insensitive to MAPK inhibitors because of the induction of the prosurvival AKT pathway. Thus, we treated AP1510- and EGF-stimulated cells in 3D Matrigel with the dual PI3K/mTOR inhibitor BEZ-235 (41) and MEK1/2 inhibitor CI-1040 (42). Treatment with CI-1040 completely inhibited AP1510- but not EGF-induced FKBP–HA acinus formation. BEZ-235 blocked EGF- and AP1510-stimulated cell growth (Fig. 4C and D). Consistent with these data, CI-1040

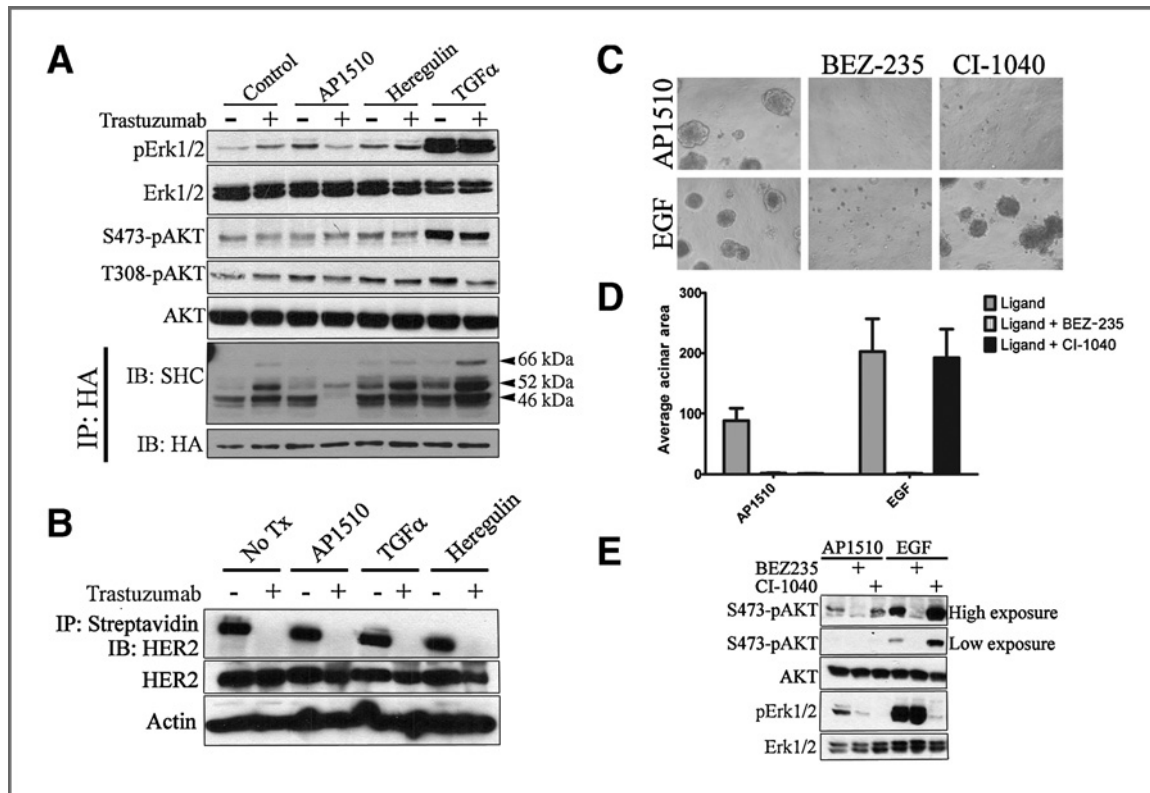


**Figure 4.** Trastuzumab blocks HER2 homodimer- but not heterodimer-induced pErk1/2. **A**, cells were treated with AP1510, TGF $\alpha$ , or heregulin  $\pm$  trastuzumab (20  $\mu$ g/mL) for 1 hour. Protein lysates were prepared and subjected to SDS-PAGE and immunoblot analyses with the indicated antibodies. Bottom two panels, HER2-FKBP-HA was precipitated with an HA antibody; immune complexes were separated by SDS-PAGE, transferred to nitrocellulose membranes, and then subjected to immunoblot analysis with an Shc or an HA antibody (control). **B**, trastuzumab-induced downregulation of HER2. FKBP-HA cells were treated with AP1510, TGF $\alpha$ , or heregulin  $\pm$  trastuzumab overnight and then biotinylated as described in Materials and Methods. Cell lysates were precipitated with immobilized Neutravidin gel; elutes were separated by SDS-PAGE and subjected to HER2 immunoblot. Bottom two panels, HER2 and actin immunoblots of whole cell lysates to control for gel loading in the top panel. **C**, 3D Matrigel growth assays with FKBP-HA cells induced with AP1510 or EGF for 14 days in the presence or absence of NVPBEZ-235 or CI-1040. Media, ligands, and inhibitors were replenished every 3 days. **D**, average acinar area in 5 randomly chosen fields per well was quantified with the ImageJ software. Each bar represents the mean acinar area  $\pm$  SD ( $n = 4$ ). **E**, protein lysates from cells treated for 1 hour with AP1510 or EGF  $\pm$  BEZ-235 or  $\pm$  CI-1040 as indicated were subjected to SDS-PAGE followed with immunoblotting with antibodies shown on the left of each panel.

inhibited pErk1/2 in both AP1510- and EGF-induced cells whereas BEZ-235 blocked EGF-induced as well as basal pAKT (Fig. 4E). Although AP1510-induced growth is driven by Erk1/2 activity, we believe that blocking the prosurvival PI3K/AKT pathway by BEZ-235 is sufficient to suppress growth in the absence of any compensatory upregulation of pErk1/2. Although it is possible that the inhibition of mTOR also plays a role in suppressing AP1510-induced growth by BEZ-235, we chose the drug to ensure complete inhibition of the PI3K/AKT/mTOR network. Such a strategy may minimize the possibility of PI3K pathway reactivation (41). These results suggest that the increased sensitivity of HER2 homodimer-driven growth to trastuzumab can be attributed to selective inhibition of Erk1/2 and low levels of active AKT.

#### High HER2 homodimer levels correlate with response to trastuzumab

We expanded our study to measure levels of HER2-containing homo- and heterodimers in a panel of 3 trastuzu-

mal-sensitive and 5 trastuzumab-resistant breast cancer cell lines with *HER2* gene amplification (Supplementary Table 2). We employed a fluorescent antibody-based proximity assay (VeraTag). This assay can quantify protein-protein interactions in formalin-fixed, paraffin-embedded (FFPE) cell pellet or tissue sections and involves the use of 2 HER2 monoclonal antibodies, one conjugated to a fluorescent reporter tag and the other linked to a photosensitizer molecule. Photoactivation with UV light results in the photosensitizer generating singlet oxygen, which then cleaves the fluorescent tag on the second antibody. The sphere of influence of the singlet oxygen is limited by the proximity of receptors to which the antibodies are directed (25). The cleaved fluorescent tag can then be quantified using capillary electrophoresis and used as an indicator of levels of protein-protein interaction. Using this assay, we confirmed that HER2 homodimers were induced only in AP1510-treated but not TGF $\alpha$ - or heregulin-treated, formalin-fixed FKBP-HA cells (Fig. 5A).



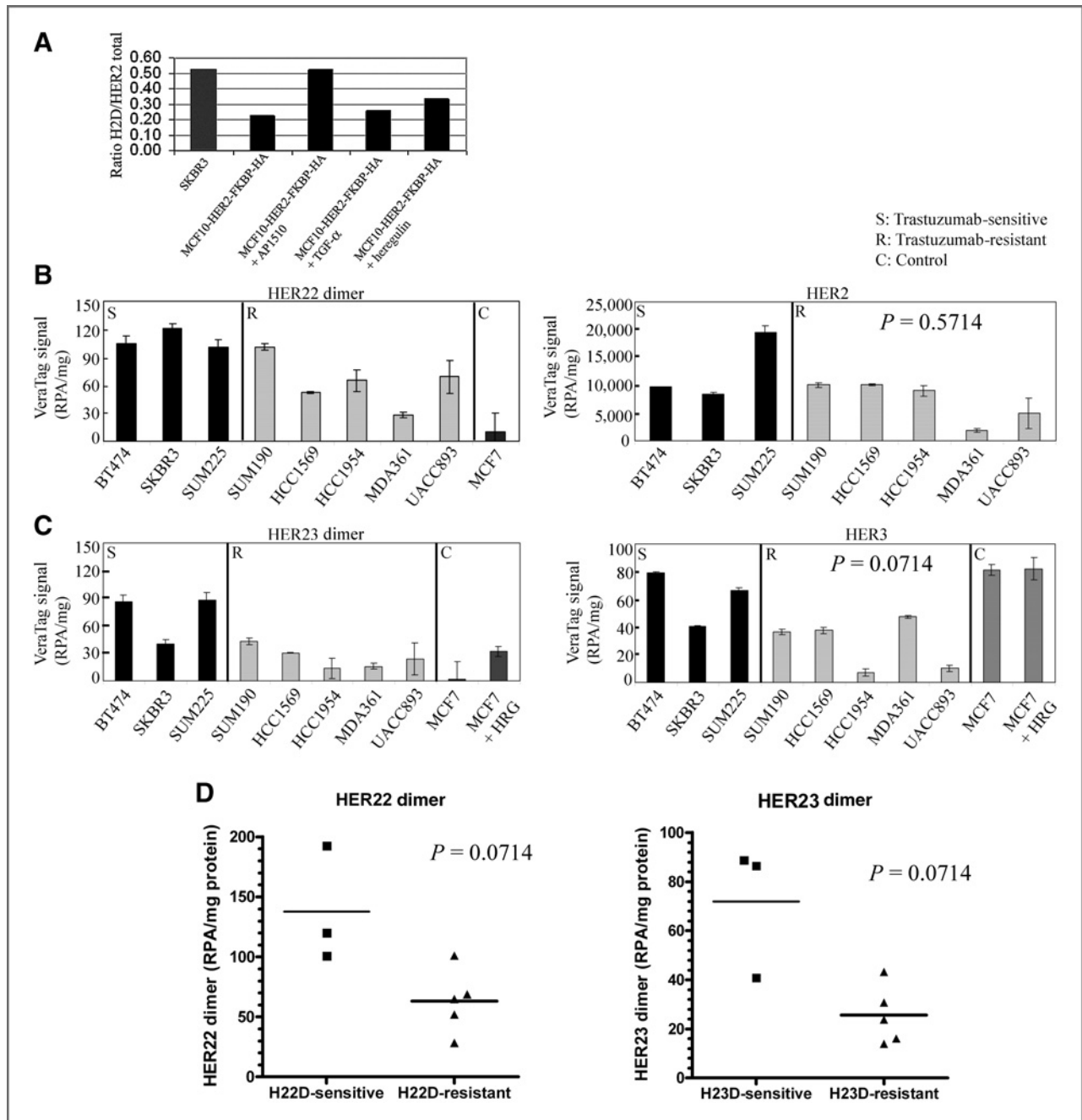


**Figure 5.** HER2-containing dimer levels in HER2<sup>+</sup> breast cancer cell lines. **A**, fluorescent antibody-based proximity (VeraTag) assay to confirm receptor ligand-induced HER2 homodimers (HER22). Cells were treated with AP1510, TGF $\alpha$ , or heregulin for 15 minutes; formalin-fixed cell pellets were prepared as indicated in Materials and Methods. SKBR3 cells, which exhibit *HER2* gene amplification (7), were used as positive controls. **B**, lysates from the indicated cell lines were subjected to the VeraTag assay to measure HER2 homodimers and total HER2. MCF7 cells, with a single copy of HER2, were used as a negative control. **C**, lysates from the indicated cell lines were subjected to the VeraTag assay to measure HER2/HER3 heterodimers (HER23) and total HER3. MCF7 cells treated with heregulin were used as a positive control for HER2/HER3 dimer formation. **D**, nonparametric *t* test (Mann-Whitney) to compare HER2-containing dimer formation between trastuzumab-sensitive and -resistant lines.

There was a trend for higher levels of HER2/HER2 homodimer (HER22) in trastuzumab-sensitive lines compared with the resistant lines [ $P = 0.07$ ; Fig. 5B (left) and D (left)]. We realize that this is a small sample size and as such the power

from the number of cell lines studied may not be enough for any difference in dimer levels to achieve statistical significance. Interestingly, we also observed a trend for higher total HER3 ( $P = 0.07$ ) and ligand-independent HER2/HER3 heterodimer



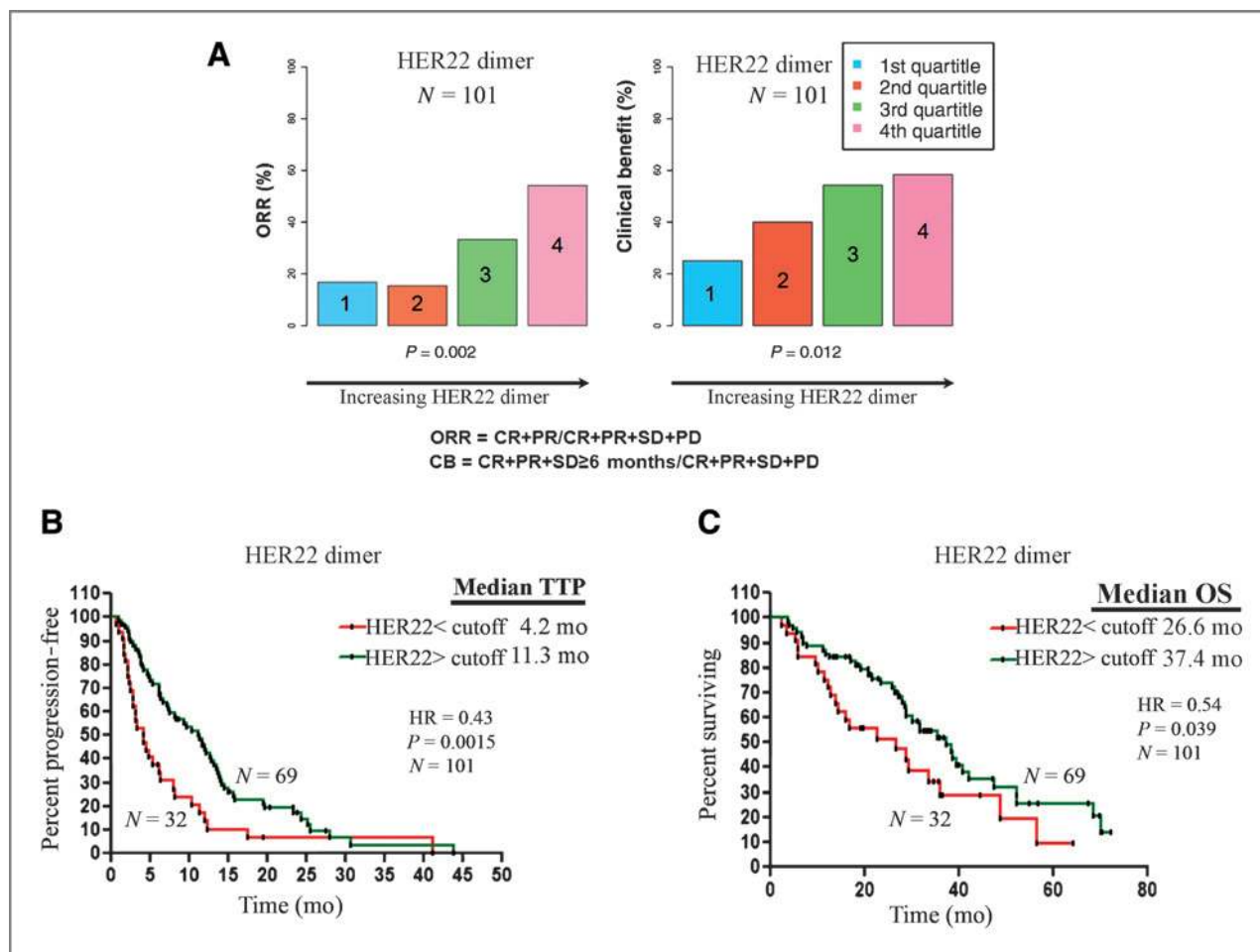


**Figure 6.** High HER2 homodimer levels correlate with response to trastuzumab. **A**, tumor sections from paraffin blocks of HER2<sup>+</sup> primary tumors were subjected to the VeraTag assay as indicated in Materials and Methods. Patients were divided into 4 groups on the basis of quartiles of measured HER2 homodimer (HER22) levels. ORR and CB were calculated for each subgroup of patients. CR, complete response; PR, partial response; SD, stable disease; PD, progressive disease. **B**, univariate KM analysis examining TTP using HER22. Cutoffs were determined by positional scanning and used to differentiate high HER22 from low HER22. **C**, univariate KM analysis examining OS using HER22. Cutoffs determined in **B** were used in **C**.

(HER23;  $P = 0.07$ ) levels in sensitive lines than in resistant lines (Fig. 5C and D, right). This observation points to the possibility that in these 3 sensitive lines (BT474, SKBR3, and SUM225), trastuzumab blocks the high levels of both HER22 dimers and ligand-independent HER23 dimers (43).

Finally, we employed this assay to quantify levels of HER22 dimers in FFPE sections from HER2-overexpressing primary breast cancers that had been treated with trastuzumab and for which outcome data were available (Table 1). Patients were sorted into 4 groups according to quartiles of measured HER22. Overall response rate (ORR) and clinical benefit (CB) were calculated for each subgroup of patients as outcome measures (Fig. 6A). In both analyses, a statistically significant trend favoring better responses at higher levels of HER22 (test for trend  $P = 0.002$  for ORR and  $P = 0.012$  for CB) was observed. Univariate Kaplan-Meier (KM) analyses examining TTP were done. Cutoffs determined by positional scanning were used to discriminate "high" from "low" HER22 ( $\geq$ HER22

vs.  $<$ HER22 = 2.5). Statistically significant relationships were observed with those patients exhibiting higher levels of HER22 (HR = 0.43;  $P = 0.0015$ ) experiencing longer TTP than those patients with lower HER22 (Fig. 6B). Median TTP was 4.2 and 11.3 months for the subgroups with HER22 values below and above the cutoff, respectively. Univariate KM analyses were also done using overall survival (OS) as the outcome end point (Fig. 6C). Patients with higher levels of HER22 exhibited a median OS of 37.4 months versus 26.6 months in those with HER22 levels below the cutoff (HR = 0.54;  $P = 0.039$ ).

## Discussion

In tumors with *HER2* gene amplification, activation of HER2 network results in downstream activation of PI3K/AKT (9) and MAPK (10). The HER2 antibody trastuzumab has changed the natural history of breast cancer overall. However, many patients with *HER2* gene-amplified tumors do not respond

or eventually progress after therapy with trastuzumab (14, 44), thus suggesting the presence of *de novo* and acquired mechanisms of drug resistance. Coexistent mutational alterations in PI3K/AKT pathway have been associated with a lower response to trastuzumab in preclinical and retrospective clinical cohorts (16, 17). HER2<sup>+</sup> tumors with high levels of HER2 C-terminal fragments that lack the trastuzumab-binding epitope have also been reported to be resistant to trastuzumab (45). Despite these important leads, there is no widely used biomarker(s) that can reliably predict lack of benefit from trastuzumab in patients bearing HER2-overexpressing tumors.

In this study, we developed a cell-based model in which we conditionally regulated activation of the ErbB network (Fig. 1). Using this model, we identified distinct transcriptional and signaling profiles induced by activation of HER2-containing homo- and heterodimers (Fig. 3). HER2 homodimers activated predominantly the MAPK but not the PI3K/AKT pathway (Fig. 3; Supplementary Figs. 1 and 2). Likely as a result of the high levels of EGFR in MCF10A cells (46) used to generate the FKBP-HA cells, the EGFR ligand TGF $\alpha$  induced a broader signaling spectrum than AP1510 (Fig. 3; Supplementary Figs. 1 and 2). Furthermore, gene expression induced by the EGFR ligand was associated with a recently reported poor prognosis signature in patients bearing HER2-overexpressing breast cancers (27).

All ligands used in this study, AP1510, TGF $\alpha$  (or EGF), and heregulin, stimulated FKBP-HA cell growth. Interestingly, trastuzumab was only effective at inhibiting AP1510-stimulated, HER2 homodimer-induced cell growth (Fig. 2). This action correlated with the ability of trastuzumab to induce dissociation of Shc from HER2 homodimers and subsequent inhibition of pErk1/2 (Fig. 4A). This is consistent with earlier reports supporting trastuzumab-mediated inhibition of both cell growth and Erk1/2 in cell lines (47). Furthermore, published clinical data from Mohsin and colleagues have shown that in HER2-overexpressing primary human tumors, levels of pErk1/2 but not pAKT as assessed by immunohistochemistry of tumor sections are reduced by treatment with trastuzumab given alone (48). Of note, TGF $\alpha$ - and heregulin-induced Erk1/2 activation was resistant to trastuzumab. Moreover, HER2 heterodimer-induced growth was resistant to the MEK inhibitor CI-1040 (Fig. 4C and D), likely due to the simultaneous activation of AKT, which was not observed with AP1510. These data also suggest that HER2 homodimer-induced growth is sensitive to trastuzumab because of the inability of these dimers to potentially activate the prosurvival AKT pathway. These results imply that because of the more limited signaling output, HER2<sup>+</sup> tumors with high levels of HER2 homodimers may exhibit a better outcome than tumors in which HER2 is predomi-

nantly in a hetero-oligomeric conformation as supported by the data shown in Supplementary Fig. 4.

An implication of these results is that clinically applicable assays that measure the oligomeric conformations of HER2 in HER2<sup>+</sup> tumors will help predict the odds of response to trastuzumab. Indeed, in a cohort of patients bearing metastatic HER2-overexpressing breast cancer, higher HER2 homodimer levels measured with a proximity-based, antibody-dependent HER2 dimer detection assay correlated with better clinical outcome following therapy with trastuzumab and chemotherapy (Fig. 6). We realize that the results of this analysis are limited by the small size of the patient cohort, the retrospective nature of the study, and the heterogeneous chemotherapy with which patients were treated. Furthermore, the cutoff value used to distinguish between high and low HER2 homodimer levels applied to the outcome analysis was derived from the same cohort. As such, the observed relationships and derived cutoff values will require validation in an independent cohort before being regarded as widely useful. However, consistent with our observations from *in vitro* experiments, this data set suggests that trastuzumab has preferential activity against tumors driven predominantly by HER2 homodimer-induced signaling. Whether the converse is true with assays measuring HER2-containing heterodimers will require further investigation.

## Disclosure of Potential Conflicts of Interest

No potential conflicts of interest were disclosed.

## Acknowledgments

We are grateful to Weidong Huang, Jodi Weidler, Yolanda Lie, Thomas Sherwood, and Gordon Parry from Monogram Biosciences for help with the manuscript.

## Grant Support

This work was supported by R01 grant CA80195 (C.L. Arteaga), ACS Clinical Research Professorship Grant CRP-07-234 (C.L. Arteaga), The Lee Jeans Translational Breast Cancer Research Program (C.L. Arteaga), Breast Cancer Specialized Program of Research Excellence (SPORE) P50 CA98131, Vanderbilt-Ingram Cancer Center Support Grant P30 CA68485, U54 CA112970 (G.B. Mills), and a Stand Up to Cancer/ American Association for Cancer Research Dream Team Translational Cancer Research Grant, (Grant No. SU2C-AACR-DT0209) (C.L. Arteaga, G.B. Mills). R. Ghosh is partially supported by a postdoctoral research award (W81XWH-09-1-0474) from DOD Breast Cancer Research Program.

The costs of publication of this article were defrayed in part by the payment of page charges. This article must therefore be hereby marked *advertisement* in accordance with 18 U.S.C. Section 1734 solely to indicate this fact.

Received June 17, 2010; revised November 16, 2010; accepted November 29, 2010; published OnlineFirst February 15, 2011.

## References

1. Sliwkowski Y. Untangling the ErbB signaling network. *Nat Rev Mol Cell Biol* 2001;2:127-37.
2. Yarden A. The ErbB signaling network in embryogenesis and oncogenesis: signal diversification through combinatorial ligand-receptor interactions. *FEBS Lett* 1997;410:83-6.
3. Burden S, Yarden Y. Neuregulins and their receptors: a versatile signaling module in organogenesis and oncogenesis. *Neuron* 1997;18:847-55.
4. Stern DF. The biology of erbB-2/neu/HER-2 and its role in cancer. *Biochim Biophys Acta* 1994;198:165-84.
5. Ross JS, Fletcher JA. The HER-2/neu oncogene in breast cancer: prognostic factor, predictive factor, and target for therapy. *Stem Cells* 1998;16:413-28.
6. Landgraf R. HER2 therapy. HER2 (ERBB2): functional diversity from structurally conserved building blocks. *Breast Cancer Res* 2007;1:202.

7. Worthylake R, Opresko LK, Wiley HS. ErbB-2 amplification inhibits down-regulation and induces constitutive activation of both ErbB-2 and epidermal growth factor receptors. *J Biol Chem* 1999;274:8865–74.
8. Graus-Porta D, Beerli RR, Daly JM, Hynes NE. ErbB2, the preferred heterodimerization partner of all ErbB receptors, is a mediator of lateral signaling. 1997;16:1647–55.
9. Hsieh AC, Moasser MM. Targeting HER proteins in cancer therapy and the role of the non-target HER3. *Br J Cancer* 2007;97:453–7.
10. Dankort D, Maslikowski B, Warner N, Kanno N, Kim H, Wang Z, et al. Grb2 and Shc adapter proteins play distinct roles in Neu (ErbB-2)-induced mammary tumorigenesis: implications for human breast cancer. *Mol Cell Biol* 2001;21:1540–51.
11. Carter Pea. Humanization of an anti-p185HER2 antibody for human cancer therapy. *Proc Natl Acad Sci U S A* 1992;89:4285–9.
12. Medina PJ, Goodin S. Lapatinib: a dual inhibitor of human epidermal growth factor receptor tyrosine kinases. *Clin Ther* 2008;30:1426–47.
13. Vogel CL, Cobleigh MA, Tripathy D, Gutheil JC, Harris LN, Fehrenbacher L, et al. Efficacy and safety of trastuzumab as a single agent in first-line treatment of HER2-overexpressing metastatic breast cancer. *J Clin Oncol* 2002;20:719–26.
14. Slamon DJ, Leyland-Jones B, Shak S, Fuchs H, Paton V, Bajamonde A, et al. Use of chemotherapy plus a monoclonal antibody against HER2 for metastatic breast cancer that overexpress HER2. *New Engl J Med* 2001;344:783–92.
15. Nahta R, Yu D, Huang M-C, Hortobagyi GN, Esteva FJ. Mechanisms of disease: understanding resistance to HER2-targeted therapy in human breast cancer. *Nat Clin Pract Oncol* 2006;3:269–80.
16. Nagata Y, Lan KH, Zhou X, Tan M, Esteva FJ, Sahin AA, et al. PTEN activation contributes to tumor inhibition by trastuzumab, and loss of PTEN predicts trastuzumab resistance in patients. *Cancer Cell* 2004;6:117–27.
17. Berns K, Horlings HM, Hennessy BT, Madiredjo M, Hijmans EM, Beelen K, et al. A functional genetic approach identifies the PI3K pathway as a major determinant of trastuzumab resistance in breast cancer. *Cancer Cell* 2007;12:395–402.
18. Ritter CA, Perez-Torres M, Rinehart C, Guix M, Dugger T, Engelman JA, et al. Human breast cancer cells selected for resistance to trastuzumab *in vivo* overexpress epidermal growth factor receptor and ErbB ligands and remain dependent on the ErbB receptor network. *Clin Cancer Res* 2007;13:4909–19.
19. Agus DB, Akita RW, Fox WD, Lewis GD, Higgins B, Pisacane PI, et al. Targeting ligand-activated ErbB2 signaling inhibits breast and prostate tumor growth. *Cancer Cell* 2002;2:127–37.
20. Cho HS, Mason K, Ramyar KX, Stanley AM, Gabelli SB, Denney DW Jr, et al. Structure of the extracellular region of HER2 alone and in complex with the herceptin Fab. *Nature* 2003;421:756–60.
21. Muthuswamy SK, Gilman M, Brugge JS. Controlled dimerization of ErbB receptors provides evidence for differential signaling by homo- and heterodimers. *Mol Cell Biol* 1999;19:6845–57.
22. Wang SE, Narasanna A, Perez-Torres M, Xiang B, Wu FY, Yang S, et al. HER2 kinase domain mutation results in constitutive phosphorylation and activation of HER2 and EGFR and resistance to EGFR tyrosine kinase inhibitors. *Cancer Cell* 2006;10:25–38.
23. Debnath J, Muthuswamy SK, Brugge JS. Morphogenesis and oncogenesis of MCF-10A mammary epithelial acini grown in three-dimensional basement membrane cultures. *Methods* 2003;30:256–68.
24. Penuel E, Akita RW, Sliwkowski MX. Identification of a region within the ErbB2/HER2 intracellular domain that is necessary for ligand-independent association. *J Biol Chem* 2002;277:28468–73.
25. Shi Y, Huang W, Tan Y, Jin X, Dua R, Penuel E, et al. A novel proximity assay for the detection of proteins and protein complexes: quantitation of HER1 and HER2 total protein expression and homodimerization in formalin-fixed, paraffin-embedded cell lines and breast cancer tissue. *Diagn Mol Pathol* 2009;18:11–21.
26. Engelman JA, Jänne PA, Mermel C, Pearlberg J, Mukohara T, Fleet C, et al. ErbB-3 mediates phosphoinositide 3-kinase activity in gefitinib-sensitive non-small cell lung cancer cell lines. *Proc Natl Acad Sci U S A* 2005;102:3788–93.
27. Staaf J, Ringné M, Vallon-Christersson J, Jönsson G, Bendahl PO, Holm K, et al. Identification of subtypes in human epidermal growth factor receptor 2-positive breast cancer reveals a gene signature prognostic of outcome. *J Clin Oncol* 2010;28:1813–20.
28. Hennessy BT, Lu Y, Poradosu E, Yu Q, Yu S, Hall H, et al. Pharmacodynamic markers of perifosine efficacy. *Clin Cancer Res* 2007;13:7421–31.
29. Hu J, He X, Baggerly KA, Coombes KR, Hennessy BT, Mills GB. Non-parametric quantification of protein lysate arrays. *Bioinformatics* 2007;23:1986–94.
30. Tibes R, Qiu Y, Lu Y, Hennessy B, Andreeff M, Mills GB, et al. Reverse phase protein array: validation of a novel proteomic technology and utility for analysis of primary leukemia specimens and hematopoietic stem cells. *Mol Cancer Ther* 2006;5:2512–21.
31. Köstler WJ, Schwab B, Singer CF, Neumann R, Rücklinger E, Brodowicz T, et al. Monitoring of serum Her-2/neu predicts response and progression-free survival to trastuzumab-based treatment in patients with metastatic breast cancer. *Clin Cancer Res* 2004;10:1618–24.
32. Mailloux AA, Overholtzer M, Schmelzle T, Bouillet P, Strasser A, Brugge JS. BIM regulates apoptosis during mammary ductal morphogenesis, and its absence reveals alternative cell death mechanisms. 2007;12:221–34.
33. Badache A, Hynes NE. A new therapeutic antibody masks ErbB2 to its partners. *Cancer Cell* 2004;5:299–301.
34. Liu H, Tarima S, Borders AS, Getchell TV, Getchell ML, Stromberg AJ. Quadratic regression analysis for gene discovery and pattern recognition for non-cyclic short time-course microarray experiments. *BMC Bioinformatics* 2005;6:106.
35. Chen Y, Guggisberg N, Jorda M, Gonzalez-Angulo A, Hennessy B, Mills GB, et al. Combined Src and aromatase inhibition impairs human breast cancer growth *in vivo* and bypass pathways are activated in AZD0530-resistant tumors. *Clin Cancer Res* 2009;15:3396–405.
36. Ishizawa R, Miyake T, Parsons S. c-Src modulates ErbB2 and ErbB3 heterocomplex formation and function. *Oncogene* 2006;26:3503–10.
37. Ratna KV, Aysegul AS, Liana A, Rui-An W, Rakesh K. Heregulin and HER2 signaling selectively activates c-Src phosphorylation at tyrosine 215. *FEBS Lett* 2003;543:76–80.
38. Huang X, Gao L, Wang S, McManaman JL, Thor AD, Yang X, et al. Heterotrimerization of the growth factor receptors erbB2, erbB3, and Insulin-like growth factor-1 receptor in breast cancer cells resistant to herceptin. *Cancer Res* 2010;70:1204–14.
39. Pines J, Hunter T. Human cyclin A is adenovirus E1A-associated protein p60 and behaves differently from cyclin B. *Nature* 1990;346:760–3.
40. Aaltonen K, Amini RM, Heikkilä P, Aittomäki K, Tamminen A, Nevanlinna H, et al. High cyclin B1 expression is associated with poor survival in breast cancer. *Br J Cancer* 2009;100:1055–60.
41. Maira SM, Stauffer F, Brueggen J, Furet P, Schnell C, Fritsch C, et al. Identification and characterization of NVP-BE2253, a new orally available dual phosphatidylinositol 3-kinase/mammalian target of rapamycin inhibitor with potent *in vivo* antitumor activity. *Mol Cancer Ther* 2008;7:1851–63.
42. Sebolt-Leopold JS, Dudley DT, Herrera R, Van Becelaere K, Wiland A, Gowan RC, et al. Blockade of the MAP kinase pathway suppresses growth of colon tumors *in vivo*. *Nat Med* 1999;5:810–6.
43. Junttila TT, Akita RW, Parsons K, Fields C, Lewis Phillips GD, Friedman LS, et al. Ligand-independent HER2/HER3/PI3K complex is disrupted by trastuzumab and is effectively inhibited by the PI3K inhibitor GDC-0941. *Cancer Cell* 2009;15:429–40.
44. Vogel C, Cobleigh MA, Tripathy D, Gutheil JC, Harris LN, Fehrenbacher L, et al. First-line, single-agent Herceptin® (trastuzumab) in metastatic breast cancer: a preliminary report. *Eur J Cancer* 2001;37:25–9.
45. Scaltriti M, Rojo F, Ocaña A, Anido J, Guzman M, Cortes J, et al. Expression of p95HER2, a truncated form of the HER2 receptor, and

- response to anti-HER2 therapies in breast cancer. *J Natl Cancer Inst* 2007;99:628–38.
46. Ciardiello F, Caputo R, Bianco R, Damiano V, Pomatico G, De Placido S, et al. Antitumor effect and potentiation of cytotoxic drug activity in human cancer cells by ZD-1839 (Iressa), an epidermal growth factor receptor-selective tyrosine kinase inhibitor. *Clin Can Res* 2000;6:2053–63.
47. Pickl M, Ries CH. Comparison of 3D and 2D tumor models reveals enhanced HER2 activation in 3D associated with an increased response to trastuzumab. *Oncogene* 2008;28:461–8.
48. Mohsin SK, Weiss HL, Gutierrez MC, Chamness GC, Schiff R, Digiovanna MP, et al. Neoadjuvant trastuzumab induces apoptosis in primary breast cancers. *J Clin Oncol* 2005;23:2460–8.



# Cancer Research

The Journal of Cancer Research (1916–1930) | The American Journal of Cancer (1931–1940)

## Trastuzumab Has Preferential Activity against Breast Cancers Driven by HER2 Homodimers

Ritwik Ghosh, Archana Narasanna, Shizhen Emily Wang, et al.

*Cancer Res* 2011;71:1871-1882. Published OnlineFirst February 15, 2011.

<b>Updated version</b>	Access the most recent version of this article at: doi: <a href="https://doi.org/10.1158/0008-5472.CAN-10-1872">10.1158/0008-5472.CAN-10-1872</a>
<b>Supplementary Material</b>	Access the most recent supplemental material at: <a href="http://cancerres.aacrjournals.org/content/suppl/2011/02/11/0008-5472.CAN-10-1872.DC1">http://cancerres.aacrjournals.org/content/suppl/2011/02/11/0008-5472.CAN-10-1872.DC1</a>

<b>Cited articles</b>	This article cites 46 articles, 17 of which you can access for free at: <a href="http://cancerres.aacrjournals.org/content/71/5/1871.full#ref-list-1">http://cancerres.aacrjournals.org/content/71/5/1871.full#ref-list-1</a>
<b>Citing articles</b>	This article has been cited by 22 HighWire-hosted articles. Access the articles at: <a href="http://cancerres.aacrjournals.org/content/71/5/1871.full#related-urls">http://cancerres.aacrjournals.org/content/71/5/1871.full#related-urls</a>

<b>E-mail alerts</b>	<a href="#">Sign up to receive free email-alerts</a> related to this article or journal.
<b>Reprints and Subscriptions</b>	To order reprints of this article or to subscribe to the journal, contact the AACR Publications Department at <a href="mailto:pubs@aacr.org">pubs@aacr.org</a> .
<b>Permissions</b>	To request permission to re-use all or part of this article, use this link <a href="http://cancerres.aacrjournals.org/content/71/5/1871">http://cancerres.aacrjournals.org/content/71/5/1871</a> . Click on "Request Permissions" which will take you to the Copyright Clearance Center's (CCC) Rightslink site.